

Available online at www.sciencedirect.com

Chinese Journal of Aeronautics 20(2007) 153-156

**Chinese
Journal of
Aeronautics**www.elsevier.com/locate/cja

The Influence of Co Addition on Phase Transformation Behavior and Mechanical Properties of TiNi Alloys

JING Rui-rui, LIU Fu-shun*

School of Materials Science and Engineering, Beijing University of Aeronautics and Astronautics, Beijing 100083, China

Received 10 August 2006; accepted 6 November 2006

Abstract

The influences of Co-addition on phase transformation behavior and mechanical properties of TiNi alloys were investigated. Results indicate that, as a substitute for Ni, Co added to TiNi alloys can dramatically decrease the martensite transformation temperature, and R phase transformation and martensite transformation are accordingly separated. When Co-content reach 10 at.%, the martensite transformation temperature is lower than that of liquid nitrogen. During deformation at room temperature, $Ti_{50}Ni_{48}Co_2$ alloy exhibits good ductility with a lower stress plateau caused by stress-induced martensite and martensite reorientation.

Keywords: TiNiCo; shape memory alloy; martensite transformation; mechanical property

1 Introduction

TiNi-based alloys have found wide application in aeronautic and medical fields because of their good mechanical properties, excellent shape memory effects, superelasticity and good bio-compatibility^[1-3]. It has been well recognized that the transformation temperature of TiNi-based alloys varies dramatically with their composition. A slight change in Ni/Ti ratio or addition of a third element can give rise to a remarkable change in transformation temperature. In addition, altering Ni/Ti ratio and adding the third element can also influence the mechanical properties of the NiTi-based alloys^[4-10]. Till now, a lot of studies have been devoted to the influences of the third element like Fe, Cu, Nb, etc., on the transformation behavior and shape memory effects and/or superelasticity^[4-6,10]. In 1971, elastic properties of TiNiCo shape memory alloy wires were evaluated by Andreasen to develop TiNi-based

TiNi-based shape memory alloys for medical application^[2]. However, phase transformation behavior and mechanical properties of TiNiCo alloy have not been reported. The present paper is aimed to fill this void.

2 Experimental Procedure

The $Ti_{50}Ni_{50-x}Co_x$ ($x=2, 4, 6, 8$ and 10) alloy ingots were produced by melting four times in a high frequency vacuum furnace and homogenized at $850\text{ }^\circ\text{C}$ for 24 h in an evacuated and sealed quartz capsule. Then these ingots were hot-worked into sheets approximately 1.5 mm in thickness for mechanical tests. Spark-cut $33\text{ mm}\times 2\text{ mm}\times 1\text{ mm}$ in a gauge dimension, the specimens for tensile tests were heat treated at $500\text{ }^\circ\text{C}$ for 1 h. The transformation behavior was studied by means of typical four terminal techniques on electrical resistivity apparatus with the heating/cooling rate of 1 K/min. X-ray diffraction (XRD) analysis was carried out on a Rigaku D/max 2200pc diffractometer. The mechanical properties were examined by tensile tests carried out

*Corresponding author. Tel.: +86-13601072308.

E-mail address: liufs@buaa.edu.cn

Foundation item: National Defence Pre-research Foundation

on a MTS model 880 at ambient temperature with a displacement rate of 1 mm/min.

3 Results and Discussion

3.1 Phase transformation behavior of TiNiCo alloys

Fig.1 shows electrical resistivity vs. temperature curves of $Ti_{50}Ni_{50-x}Co_x$ ($x=2, 4, 6, 8$ and 10) alloys. Generally, for near-equiatomic TiNi alloys, the shape memory effects and pseudoelasticity occur in association with thermoelastic martensite transformation from the high-temperature parent phase with a B2 structure to the low-temperature martensite phase with a monoclinic B19' structure, but in some cases they take place along with two step transformation: e.g., from B2 to an intermediate (R) phase with a rhombohedral B19 structure and then to B19' phase. These phenomena are quite sensitive to the structural fineness of the parent B2 phase and the factors such as Ni-content, aging, thermomechanical treatment and addition of other alloying elements, which, by affecting the structures, are important to controlling the phase transformation behavior^[11]. Among the TiNiX ternary alloys, TiNiFe and TiNiAl alloys are well known for the two step transformation^[6].

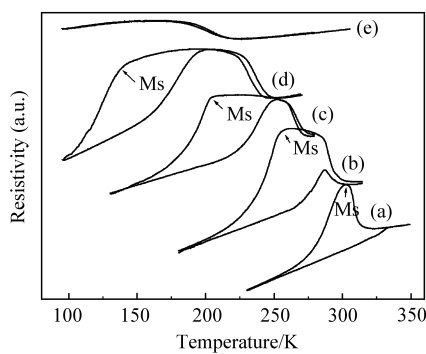


Fig.1 Electrical resistivity vs. temperature curves of TiNiCo alloys. (a) $Ti_{50}Ni_{48}Co_2$; (b) $Ti_{50}Ni_{46}Co_4$; (c) $Ti_{50}Ni_{44}Co_6$; (d) $Ti_{50}Ni_{42}Co_8$; (e) $Ti_{50}Ni_{40}Co_{10}$.

From the curves of $Ti_{50}Ni_{48}Co_2$ alloy, where the top line corresponds to cooling process and the bottom line heating one, it is easy to obtain martensite transformation temperature of about 302 K. In Fig.1(b), (c) and (d), two inflexions appear on both

cooling and heating curves, which implies R phase transformation happening prior to martensite transformation. And so the phase transformation sequence can be described as $B2 \rightarrow B19 \rightarrow B19'$ on cooling. However, the opposite is the case on heating, where exists $B19' \rightarrow B19 \rightarrow B2$. From Fig.1(e), martensite transformation temperature of $Ti_{50}Ni_{40}Co_{10}$ can not be found at the liquid nitrogen temperature.

In order to clearly showcase the phase transformation, Ms, Rs, As of $Ti_{50}Ni_{50-x}Co_x$ ($x=2, 4, 6, 8$ and 10) alloys are carefully analyzed as shown in Fig.2. The Ms temperature decreases by about 40-60 K per 2 at.% Co-addition, and Ms declines more rapidly than Rs, which induces the R phase transformation to separate from martensite phase transformation.

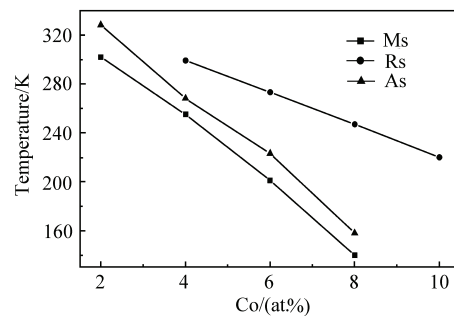


Fig.2 The characteristic transformation temperature of $Ti_{50}Ni_{50-x}Co_x$ ($x=2, 4, 6, 8$ and 10) alloys.

Fig.3 shows X-ray diffraction patterns recorded at room temperature on these alloys. As shown in Fig.3(a), the martensite phase and B2 coexist in $Ti_{50}Ni_{48}Co_2$ alloy, which accords with electrical resistivity vs. temperature curve in that the marten-

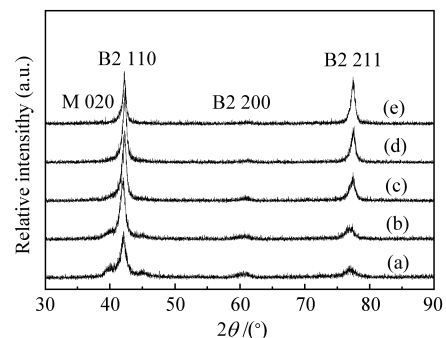


Fig.3 X-ray diffraction patterns measured at room temperature for alloys. (a) $Ti_{50}Ni_{48}Co_2$; (b) $Ti_{50}Ni_{46}Co_4$; (c) $Ti_{50}Ni_{44}Co_6$; (d) $Ti_{50}Ni_{42}Co_8$ and (e) $Ti_{50}Ni_{40}Co_{10}$.

site transform of $\text{Ti}_{50}\text{Ni}_{48}\text{Co}_2$ alloy starts but does not finish completely at room temperature, and that the weak peak of martensite can be ascribed to the transformation from B2 to B19' phase bringing about a few martensite phases. In contrast to $\text{Ti}_{50}\text{Ni}_{48}\text{Co}_2$ alloy, only B2 parent phase exists in Fig. 3(b), 3(c), 3(d) and 3(e) because of their lower phase transformation temperatures.

3.2 Mechanical properties of $\text{Ti}_{50}\text{Ni}_{50-x}\text{Co}_x$ ($x=2, 4, 6, 8$ and 10) shape memory alloys

In order to investigate the mechanical properties of $\text{Ti}_{50}\text{Ni}_{50-x}\text{Co}_x$ ($x=2, 4, 6, 8$ and 10) shape memory alloys, tensile tests were conducted at room temperature and the typical stress vs. strain curves obtained are shown in Fig.4. The curves of stress vs. strain are different from each other because of diversified initial states of the specimens at the testing temperature. The curve of $\text{Ti}_{50}\text{Ni}_{48}\text{Co}_2$ shows the process of deformation in a mixture state of B2 plus martensite from stress-induced B2→B19 transformation to martensite reorientation followed by plastic deformation. The deformation induced by stress-induced martensite and martensite reorientation results in a Lüders-like behavior. The Lüders-like deformation ends up at a tensile strain of 5% when the deformation process develops into a uniform stage characterized by a quickly increasing stress. The best fracture elongation rate of more than

20% has been found in $\text{Ti}_{50}\text{Ni}_{48}\text{Co}_2$ alloy.

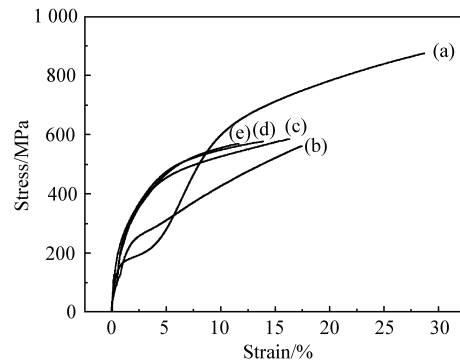


Fig.4 Stress vs. strain curves for alloys. (a) $\text{Ti}_{50}\text{Ni}_{48}\text{Co}_2$; (b) $\text{Ti}_{50}\text{Ni}_{46}\text{Co}_4$; (c) $\text{Ti}_{50}\text{Ni}_{44}\text{Co}_6$; (d) $\text{Ti}_{50}\text{Ni}_{42}\text{Co}_8$ and (e) $\text{Ti}_{50}\text{Ni}_{40}\text{Co}_{10}$.

In Fig.4, The stress vs. strain curves of other four alloys exhibit general plastic deformation of B2 parent phase and the stress plateau associated with stress-induced martensite, and martensite reorientation is no longer observed. The different deformation processes of TiNiCo alloys are caused by the different loading temperatures and phase transformation temperatures. The M_s points of the four alloys are lower than their loading temperatures, which implies the absence of plateaus. As for TiNiCo alloys, from Table 1, the yield strength (σ_s) has a slight increase from 177 MPa to 275 MPa with Co-addition from 2 at.% to 10 at.%. The fracture strength (σ_b) of B2 phase also increases from 561 MPa to 575 MPa.

Table 1 σ_s , σ_b and elongation rate of $\text{Ti}_{50}\text{Ni}_{50-x}\text{Co}_x$ ($x=2, 4, 6, 8$ and 10)

| | $\text{Ti}_{50}\text{Ni}_{48}\text{Co}_2$ | $\text{Ti}_{50}\text{Ni}_{46}\text{Co}_4$ | $\text{Ti}_{50}\text{Ni}_{44}\text{Co}_6$ | $\text{Ti}_{50}\text{Ni}_{42}\text{Co}_8$ | $\text{Ti}_{50}\text{Ni}_{40}\text{Co}_{10}$ |
|-------------------|---|---|---|---|--|
| σ_s /MPa | 177 | 232 | 265 | 269 | 275 |
| σ_b /MPa | 841 | 561 | 566 | 568 | 575 |
| Elongation rate/% | 28.7 | 17.4 | 16.3 | 13.6 | 11.8 |

4 Conclusions

$\text{Ti}_{50}\text{Ni}_{50-x}\text{Co}_x$ ($x=2, 4, 6, 8$ and 10) alloys exhibit two-step transformation behavior since different amounts of decline of R phase and martensite transformation temperature that are induced by Co-addition result in separation of R phase transformation from martensite transformation. $\text{Ti}_{50}\text{Ni}_{50-x}\text{Co}_x$ ($x=2,$

4, 6, 8 and 10) alloys appear in different phases at room temperature, which causes different deformation processes. Moreover, the yield strength improves with Co-addition.

References

- [1] Liu F S, Ding Z, Li Y, et al. Phase transformation behaviors and mechanical properties of TiNiMo shape memory alloys. Internet-

- alloys 2005; 13: 357-360.
- [2] Zheng Y F, Zhao L C. NiTi alloys applied in the medical field. Beijing: Science Press, 2004. [in Chinese]
- [3] Jiang C B, Xu H B. Effect of pre-deformation on hysteresis in TiNiFe shape memory alloys. *Material Science Forum* 2000; 327-328: 111-114.
- [4] Xu H B, Jiang C B, Gong S K. Martensitic transformation of the $Ti_{50}Ni_{48}Fe_2$ alloy deformed at different temperatures. *Material Science Engineering* 2000; 218 (A): 234-238.
- [5] Craciunescu C M, Li J, Wuttig M. Constrained martensitic transformations in TiNiCu films. *Thin Solid Films* 2003; 434(1-2): 271-275.
- [6] Xu Z Y. Shape memory materials. Shanghai: Shanghai Jiaotong University Press, 2000. [in Chinese]
- [7] Favier D, Liu Y N. Restoration by rapid overheating of thermally stabilised martensite of NiTi shape memory alloys. *Journal of Alloys and Compounds* 2000; 297(1-2): 114-121.
- [8] Lin H C, Wu S K. The tensile behavior of a cold-rolled and reverse-transformed equiatomic TiNi alloy. *Acta Metallurgica et Materialia* 1994; 42(5):1623-1630.
- [9] Marquina M L, Jimenez M, Marquina V, et al. Structural transitions in a TiNiFe shape memory alloy. *Materials Characterization* 1994; 32(3): 189-193.
- [10] Hwang C M, Meichle M, Salamon M B, et al. Transformation behaviors of a $Ti_{50}Ni_{47}Fe_3$ alloy subsequent premartensitic behavior and the commensurate phase. *Philosophical Magazine A* 1983; 47(9): 31-36.
- [11] Otsuka K, Wayman C M. Shape memory materials. Cambridge: Cambridge University Press, 1998.